Geosci. Model Dev. Discuss., 8, 10411–10454, 2015
www.geosci-model-dev-discuss.net/8/10411/2015/
doi:10.5194/gmdd-8-10411-2015

Geoscientific Model Development Discussions

An integrated Dissolved Organic Carbon Dynamics Model (DOCDM 1.0): model development and a case study in the Alaskan Yukon River Basin

X. Lu[1,a] **and Q. Zhuang**[1,2]

[1]Department of Earth, Atmospheric, Planetary Sciences, Purdue University, West Lafayette IN, 47907, USA
[2]Department of Agronomy, Purdue University, West Lafayette, 47907, USA
[a]now at: The Ecosystems Center, the Marine Biological Laboratory, Woods Hole, MA, 02536, USA

Received: 28 September 2015 – Accepted: 8 November 2015 – Published: 10 December 2015

Correspondence to: Q. Zhuang (qzhuang@purdue.edu)

Published by Copernicus Publications on behalf of the European Geosciences Union.

Abstract

Quantitative understanding of the variation in dissolved organic carbon (DOC) is important to studying the terrestrial ecosystem carbon cycle. This study presents a process-based, dissolved organic carbon dynamics model (DOCDM 1.0) that couples the soil heat conduction, water flow, DOC production, mineralization and transport in both surface and subsurface of soil profile to quantify DOC dynamics in boreal terrestrial ecosystems. The model is first evaluated and then applied for a watershed in Alaska to investigate its DOC production and transport. We find that 42 and 27 % of precipitation infiltrates to soils in 2004, a warmer year, and in 1976, a colder year, respectively. Under warming conditions, DOC transported via overland flow does not show the expected decrease trend while the overland DOC yield shows a 4 % increase. The horizontal subsurface flow only accounts for 1–2 % of total water flux, but transports 30–50 % of DOC into rivers. Water flush due to water infiltration controls DOC transport. Snowmelt plays a noticeable role in DOC flush-out and DOC transport significantly depends on flowpaths in the study region. High soil temperature stimulates DOC production. The overland DOC export does not necessarily follow the DOC downward trend in surface water transport. Overall, this study shows that DOC export behavior is complex under changing temperature and hydrological conditions in cold-region watersheds. To adequately quantify DOC dynamics in northern high latitudes, more DOC and hydrological data are needed to better parameterize and test the developed model before extrapolating it to the region.

1 Introduction

Dynamics of dissolved organic carbon (DOC) are a critical, yet often neglected component of the terrestrial carbon cycle. The significance of DOC has been stressed by previous studies in many aspects, including its influence on nutrient cycling (Qualls and Haines, 1991; Michalzik and Matzner, 1999), its service as a microbial energy source

(Baker et al., 2000; Raymond and Bauer, 2000) and its effects on pollutant transport (Morris and Hargreaves, 1997). High latitude ecosystems, which store about one-third of the global terrestrial organic carbon (Gorham, 1991; Moore, 2002), play a vital role in determining the future terrestrial carbon cycle including DOC dynamics, under rapidly changing climatic conditions. Dramatic changes have occurred in the arctic cryosphere, biosphere, and atmosphere (Hinzman et al., 2005; Serreze et al., 2000), resulting in higher DOC concentrations in the Arctic rivers in comparison with other major river basins on the globe (Lobbes et al., 2000; Raymond et al., 2007), and the DOC flux is expected to increase in the future (Freeman et al., 2001; Tranvik and Jansson, 2002).

While the important role of DOC in regulating C transport from terrestrial ecosystems to river systems is acknowledged, the production, loss, stabilization and release of DOC, and the interaction of these processes with external environmental variables, are still not well understood. Sorption and desorption processes are widely believed to be the dominant controlling mechanisms for DOC transport through solid soil matrices (Quails and Haines, 1992a, b). Soluble DOC may be lost in sorption process or as a result of microbial mineralization, and DOC sorbed to the soil column may rejoin water during desorption process or transformed into CO_2 via degradation. At a drainage basin scale, more hydrological, land cover, catchment characteristics and soil thermal factors should also be considered in quantifying DOC patterns in stream flow. The location and distribution of flow pathways and residence times of water are among those controls to be considered. When watersheds are in low-flow periods, predominant subsurface flows usually have low DOC concentrations presumably due to their relatively deep flowpaths in mineral layers. Rainfall and snowmelt events shift DOC transport from subsurface to surface-water system. Rising water table and increasing flow flush the DOC-rich superficial soil water to the stream channels (Hornberger et al., 1994; Dutta et al., 2006).

The DOC export from northern high latitude ecosystems has more variations due to spring snowmelt, increasing temperature, and associated permafrost thawing (Ågren et al., 2010). A large portion of the annual DOC delivery into high northern latitude

rivers occurs during the spring flush (Dittmar and Kattner, 2003; Raymond et al., 2007; Holmes et al., 2008), and the main DOC source during this relatively short period is surface litter and organic matter from shallow soil layers. Meanwhile, a warmer and wetter condition is thought to stimulate microbial activity, potentially increasing DOC production (Moore et al., 1998). In contrast, Striegl et al. (2005) suggested that the thawing of frozen soils increases the thickness of the active layer and promotes more flow pathways below organic-rich soil layers, which in turn leads to less terrestrial DOC yield under warming trends.

To investigate the controlling factors for DOC export, several DOC models have been developed (e.g., Neff and Asner, 2001; Michalzik et al., 2003; Fan et al., 2010; Xu and Saiers, 2010; Mei et al., 2012). However, most of them are one-dimensional (1-D) models that are only applied to soil columns under laboratory environment, not field conditions. The 2-dimesional (2-D) overland and subsurface transport processes, which are important in DOC transport on a watershed-scale, are usually not considered. The DOC models (Boyer et al., 1996, 2000; Futter et al., 2007; Yurova et al., 2008), which are incorporated with more hydrological and biological processes, have been successfully applied at catchment scales. However none of them has fully addressed the effects of soil thermal regimes on DOC dynamics, thus may not be suitable for northern high latitudes. The aim of this study is to develop a DOC model that is applicable for arctic and subarctic watersheds. The model is then used to study the effects of climatic changes on the DOC dynamics in an Alaskan watershed.

2 Model description

The developed DOC modeling system fully considers the effects of frozen-soil thawing on DOC variation and explicitly treats 1-D and 2-D transport behaviors of DOC. It contains four modules (Fig. 1) including: (1) land surface processes, (2) soil heat conduction, (3) water infiltration; and (4) vegetation and DOC dynamics. The land surface module calculates the water and energy balance at the ground surface at an hourly time

step. It provides ground surface temperature, throughfall and snowmelt rates, which are needed in the soil heat conduction and water infiltration modules. The soil heat and water infiltration module then estimates the soil temperature profile, soil ice content and water infiltration rate by solving soil thermal and moisture equations. Finally, the DOC production, sorption and desorption, mineralization and transport processes are modeled in the DOC dynamic module. Below we describe each module (also see the detailed information in Supplement A).

2.1 Vegetation and land surface process module

The land surface process module (Fig. 1) integrates hydrological and energy processes to simulate overland and channel flow dynamics, which drive the DOC horizontal transport. Precipitation is partitioned to rain and snow according to air temperature. Canopy layer interception is a function of leaf area index (Dickinson et al., 1986). Snow accumulation and melt are simulated when there is snow on the ground and snowfall. Snowpack is treated as a two-layer medium, and its accumulation and ablation is estimated by solving mass and energy balance equations (Andreadis et al., 2009). The energy exchange on the snowpack is modeled based on the net radiation, sensible heat carried by convection, heat advected by rainfall, evaporation, sublimation, condensation and latent heat loss or gain due to melting and refreezing. Processes such as snow accumulation and ablation, dynamics in the snow water equivalent, and meltwater yield are represented in the mass balance equation. In the snow model, snow interception (Storck et al., 2002), atmospheric stability (Anderson, 1976; Tarboton et al., 1995) and blowing snow (Bowling et al., 2004) processes are considered. Total evapotranspiration is based on the Penman–Monteith equation (Monteith, 1990) and has three components: (1) evaporation from bare soil, (2) evaporation from canopy and (3) transpiration from canopy. The vegetation module (green section of Fig. 1) provides radiation and wind speed attenuation, architectural and stomatal resistance, and roughness length to estimate snow and rain interception, evapotranspiration and root uptakes. It also provides the vegetation type information required in the DOC production estimation. The

equations within the two modules are adopted from a large-scale hydrology model, the variable infiltration capacity (VIC) model (Liang et al., 1994).

Rainfall could contribute to surface or subsurface hydrological systems through infiltration, which controls the pathway of DOC transport. In arctic regions, the soil ice directly affects infiltration and heat conduction within the soil profile (Cherkauer and Lettenmaier, 1999, 2003; Cherkauer et al., 2003).

2.2 Soil heat conduction and water infiltration module

In cold regions, soil heat conduction is affected by liquid water and ice distribution; on the other hand, infiltration and water movement in soils is also influenced by changes of ice content. In this module, heat conduction and vertical water movement are resolved at a 90 s time step. When infiltration occurs, the time step is adjusted to 1 s (red section of Fig. 1). Here we made several assumptions: (1) ice is immovable and only liquid water can move in frozen soils, (2) the influences of vapor transport on water and heat conduction can be ignored, (3) liquid flows due to thermal gradients and heat conduction by convection can be neglected; and (4) unfrozen water and the subzero temperatures of frozen soils are included in the dynamic equilibrium. Under these assumptions, water movement and heat conduction only occurs in the vertical direction and can be described with one-dimensional equations.

2.2.1 Vadose zone modeling

The one-dimensional Richards equation (Richards, 1931) is used to describe vertical water movement in both frozen and unfrozen soils:

$$\frac{\partial \theta_{\mathrm{L}}(h)}{\partial t} + \frac{\rho_{\mathrm{I}}}{\rho_{\mathrm{L}}} \cdot \frac{\partial \theta_{\mathrm{I}}(T)}{\partial t} = \frac{\partial}{\partial z}\left[K(h) \cdot \frac{\partial h}{\partial z} + K(h)\right] + S \quad (1)$$

Where θ_{L} is volume liquid water content ($\mathrm{L}^3\mathrm{L}^{-3}$), θ_{I} is volume ice content ($\mathrm{L}^3\mathrm{L}^{-3}$), t is time (T), K is hydraulic conductivity (LT^{-1}), z is the spatial coordinate positive

downward, ρ_I is the density of ice (ML^{-3}) (931 kg m^{-3}), ρ_L is the density of liquid water (ML^{-3}) (1000 kg m^{-3}), h is the capillary-pressure head (L), T is the temperature (K), and S is a sink/source term (T^{-1}) due to groundwater movement (Sect. 2.4.2).

By defining:

$$\theta = \theta_L + \frac{\rho_I}{\rho_L} \cdot \theta_I \tag{2a}$$

We have:

$$\frac{\partial \theta}{\partial t} = \frac{\partial}{\partial z}\left[K(h) \cdot \frac{\partial h}{\partial z} + K(h)\right] + S \tag{2b}$$

Equation (2b) is numerically solved (Supplement B) by using fully implicit approximation and the discretization form proposed by Celia et al. (1990). The constant head could be used as the upper boundary condition for Eq. (1) when overland exists; the amount of rainfall during no overland condition decided whether constant flux or no flux should be used. Free drainage ($Flux_{bottom} = K_{bottom}$) and no flux ($Flux_{bottom} = 0$) are the two common options for setting the lower boundary condition. We found the free drainage resulted in too much leakage and no-flux bottom, on the other hand, produced too much moisture in soil. Here we set the bottom flux is determined by $Flux_{bottom} = \varepsilon \cdot K_{bottom}$ where $0 \le \varepsilon \le 1$. In northern high latitudes, ε may increase due to permafrost degradation (Lu and Zhuang, 2011). By comparing the simulated annual flow to the measurements, we set ε as 0.21 and 0.43 for the simulations of 1976 and 2004, respectively. See the Supplement B for the detailed derivation and boundary conditions setting. The relationships between ($\frac{d\theta}{dh}$), h, and K are proposed by van Genuchten (1980):

$$\begin{cases} \theta(h) = \frac{(\theta_s - \theta_r)}{\left(1+(a\cdot|h|)^{n'}\right)^{m'}} + \theta_r \\ K(h) = K_s \frac{\left\{\left(1-(a\cdot|h|)^{n'-1}\right)\left(1+(a\cdot|h|)^{n'}\right)^{-m'}\right\}^2}{\left(1+(a\cdot|h|)^{n'}\right)^{m'/2}} \end{cases} \tag{3}$$

Where θ_s, θ_r and K_s are saturated water content (L^3L^{-3}), residual water content (L^3L^{-3}) and saturated hydraulic conductivity (LT^{-1}), respectively; a, m' and n' are model parameters, and are set as 0.0335, 0.5 and 2, respectively.

The presence of ice may significantly reduce water flow in the porous medium. The scheme of Hansson et al. (2004) is used to address the ice effect. The hydraulic conductivity for the liquid water portion of the partially frozen soil, K_f is defined as:

$$K_f(h) = 10^{-\varphi Q} \cdot K(h) \tag{4}$$

Where φ is the impedance factor (Lundin, 1990) and Q is the ratio of ice content to the total (minus the residual) water content. φ is assumed to be 7.

2.2.2 Soil heat transfer

The heat transfer in soils is modeled as:

$$\frac{\partial (C' \cdot T)}{\partial t} - L_f \cdot \rho_I \frac{\partial \theta_I}{\partial t} = \frac{\partial}{\partial z}\left(\lambda \frac{\partial T}{\partial z}\right) \tag{5}$$

where T is the soil temperature (°C) and the volumetric heat capacity of the soil, C' (J m^{-3} K^{-1}) is defined as the weighted volumetric heat capacity of the soil (C'_s), liquid water (C'_L) and ice (C'_I) phases, multiplied by their respective volumetric fractions:

$$C' = C'_s\theta_s + C'_w\theta_L + C'_I\theta_I \tag{6}$$

and L_f is the volumetric latent heat of freezing (J kg^{-1}) (approximately 3.34×10^5). ρ_I and θ_I are ice density and content, respectively. λ is soil thermal conductivity

($\mathrm{W\,m^{-1}\,K^{-1}}$). Thermal conductivity is calculated with the method in Johansen (1975):

$$\lambda = (\lambda_{\mathrm{sat}} - \lambda_{\mathrm{dry}}) \cdot \lambda_{\mathrm{e}} \tag{7a}$$

$$\lambda_{\mathrm{sat}} = \begin{cases} 0.5^{n} \cdot (7.7^{q} 2.0^{1-q})^{1-n''} & \text{unfrozen} \\ 0.5^{n} \cdot (7.7^{q} 2.0^{1-q})^{1-n''} \cdot 0.269^{\mathrm{Wu}} & \text{frozen} \end{cases} \tag{7b}$$

$$\lambda_{\mathrm{dry}} = \frac{0.17 \cdot \gamma_{\mathrm{d}} + 64.7}{2700 - 0.947 \cdot \gamma_{\mathrm{d}}} \tag{7c}$$

$$\lambda_{\mathrm{e}} = \begin{cases} \log S_{\mathrm{r}} + 1 & \text{unfrozen} \\ S_{\mathrm{r}} & \text{frozen} \end{cases} \tag{7d}$$

Where n'' is the porosity, q is the quartz content, Wu is the fractional volume of unfrozen water, γ_{d} is bulk density ($\mathrm{kg\,m^{-3}}$) and S_{r} is the fraction degree of saturation. In the above soil thermal equation, the convection of sensible heat with flowing water and uptake energy associated with root water uptake are not considered. The fraction of unfrozen water is needed in order to estimate heat capacity C' and soil thermal conductivity λ. The formula proposed by Flerchinger and Saxton (1989) is used:

$$W = W^{\mathrm{C}} \left(\left(\frac{1}{g \varphi_{\mathrm{e}}} \right) \cdot \left(\frac{L_{\mathrm{f}} \cdot T}{T + 273.16} \right) \right)^{-B_{\mathrm{P}}} \tag{8}$$

Where W is the liquid water content, W^{C} is the maximum water content, g is acceleration due to gravity, φ_{e} is the air entry potential and B_{P} is the pore-size distribution.

Similarly, the fully implicit discretization form (Hansson et al., 2004) for Eq. (5) is:

$$C_i'^{n+1,m} \cdot \frac{T_i^{n+1,m+1} - T_i^{n}}{\Delta t} - \left[L_{\mathrm{f}} \cdot \rho_{\mathrm{l}} \cdot \left(\frac{\mathrm{d}\theta_{\mathrm{l}}}{\mathrm{d}T} \right)_i^{n+1,m} \cdot \frac{T_i^{n+1,m+1} - T_i^{n+1,m}}{\Delta t} \right]$$
$$- L_{\mathrm{f}} \cdot \rho_{\mathrm{l}} \frac{(\theta_{\mathrm{l}})_i^{n+1,m} - (\theta_{\mathrm{l}})_i^{n}}{\Delta t} = \frac{\lambda_{i+1/2}^{n+1,m} \cdot \left(\frac{T_{i+1}^{n+1,m+1} - T_i^{n+1,m+1}}{\Delta z} \right) - \lambda_{i-1/2}^{n+1,m} \cdot \left(\frac{T_i^{n+1,m+1} - T_{i-1}^{n+1,m+1}}{\Delta z} \right)}{\Delta z} \tag{9}$$

Where i, Δz and T^{n} denote the spatial location, node size and the approximate value of T at the nth discrete time level, respectively, $\Delta t \equiv t^{n+1} - t^{n}$ is the time step. $\frac{\mathrm{d}\theta_{\mathrm{l}}}{\mathrm{d}T}$ is evaluated by Eq. (8). Because of the dependency of the apparent volumetric heat capacity (C') and thermal conductivity (λ) on temperature, Eq. (9) is also highly nonlinear. The same iteration scheme used for the above Richards equation is also used to linearize the two nonlinear items, and m stands for iteration level. In Eq. (9), the subscripts $i-1/2$ and $i+1/2$ represent the upper and lower grid interfaces, respectively. Hydraulic conductivity and soil thermal conductivity at grid interface is calculated using geometric averaging. Equations (1) and (5) are coupled due to their mutual dependence on water content, pressure heads and temperature. The lower boundary for Eq. (9) is set to zero thermal flux. The upper boundary condition is set to the soil surface temperature (it is iteratively solved by closing the surface energy balance) or snowpack temperature if snow exists. Supplement B lists the steps for setting these two types of boundary conditions.

2.3 DOC module

A typical convection-dispersion equation is used to characterize the DOC transport (Patankar, 1980). Three processes are considered in the DOC transport: (1) one dimensional infiltration, (2) two-dimensional overland transport; and (3) two-dimensional saturated subsurface flow transport (Fig. 1). Since most of current DOC measurements

were acquired for very large regions, it is difficult to get the DOC-related parameters for typical land cover types. In this study, we used the available data from previous studies to derive type-specific parameters for those types having no direct measurements (Supplement C). The DOC desorption and microbial production processes are treated as DOC sources, and sorption and mineralization processes are sink terms. Point processes including DOC production, mineralization, sorption and desorption processes as well as DOC infiltration and two-dimensional DOC transport processes are detailed below.

2.3.1 DOC production, mineralization, sorption and desorption

The equations in Yurova et al. (2008) are used to estimate the DOC production rate ($\mathrm{mg\,g^{-1}\,h^{-1}}$):

$$P = P_{\mathrm{basal}} \cdot Q_{10}^{(T-T_{\mathrm{basal}})/10} \tag{10}$$

$$P_{\mathrm{anp}} = P \cdot K_{\mathrm{anp}} \tag{11}$$

Where Q_{10} is the increase in metabolic rates per 10 °C increase in soil temperature (Table 1), and T_{basal} is the reference temperature (20 °C in this study) when basal rates of DOC production P_{basal} ($\mathrm{mg\,g^{-1}\,h^{-1}}$) are measured (Table 1). The fraction K_{anp} (Table 1) is used to correct the anoxic rates of DOC production on the corresponding DOC production rate (P_{anp}) under aerobic conditions. Since DOC production is highly related to the soil organic carbon pool, we use plant rooting depth to approximate soil organic carbon distribution. The DOC production rate reduces 95 % ($0.05 \cdot P_{\mathrm{basal}}$) at the depth which is not located in the organic layer.

Sorption and desorption are two key mechanisms regulating DOC stabilization and release rates. Here soluble organic carbon includes dissolved (DOC) and potentially soluble, but currently solid (PDOC). PDOC can exist as suspended particulates or in soil surface and sediment. The total concentration of DOC (C_T'''; $\mathrm{g\,cm^{-3}}$) can be calcu-

lated:

$$C_T''' = \rho_{\mathrm{b}} S + \theta_{\mathrm{L}} C''' \tag{12}$$

Where ρ_{b} is the soil bulk density ($\mathrm{g\,cm^{-3}}$), S is the absorbed, potential dissolved organic carbon (PDOC) (fraction), θ_{L} is the volumetric moisture content ($\mathrm{cm^3\,cm^{-3}}$), and C''' is the DOC concentration ($\mathrm{g\,mL^{-1}}$). The sorption and desorption processes between DOC and PDOC are modeled similar to the two-region model in Fan et al. (2010). The exchange between DOC and PDOC are represented by two schemes of sorption and desorption. One is instantaneous (PDOC1) and the other is kinetic or time-dependent (PDOC2) (van Genuchten and Wagenet, 1989):

$$\rho_{\mathrm{b}} S = \rho_{\mathrm{b}} S_1 + \rho_{\mathrm{b}} S_2 \tag{13a}$$

$$S_1 = f K_d C''' \tag{13b}$$

$$\frac{\partial S_2}{\partial t} = \frac{a \cdot J_{\mathrm{w}}}{K_{\mathrm{sat}}} \left((1-f) K_d C''' - S_2 \right) \tag{13c}$$

where S_1 and S_2 are the PDOC1 and PDOC2 sorption or desorption, respectively. f is the fraction of PDOC1 exchange sites. K_d is a linear partition coefficient between the solid and aqueous phases ($\mathrm{mL\,g^{-1}}$). a is the maximum mass transfer coefficient ($\mathrm{h^{-1}}$). J_{w} is the water flux density ($\mathrm{cm\,h^{-1}}$). K_{sat} is the saturated hydraulic conductivity ($\mathrm{cm\,h^{-1}}$).

There are three DOC or PDOC pools including DOC, PDOC1 and PDOC2. All of them are subject to mineralization. The DOC and PDOC pools have the following mineralization rates ($\mathrm{mg\,cm^{-3}\,h^{-1}}$) (Yurova et al., 2008), respectively:

$$M_{\mathrm{DOC}} = M_{\mathrm{basal}} \cdot Q_{10}^{\frac{T-T_{\mathrm{basal}}}{10}} \tag{14a}$$

$$M_{\mathrm{PDOC}} = K \cdot M_{\mathrm{basal}} \cdot Q_{10}^{\frac{T-T_{\mathrm{basal}}}{10}} \tag{14b}$$

T_{basal} is the reference rate (20 °C in this study) when basal rates of M_{basal} (h^{-1}) (Table 1) are measured. Also, the microbial mineralization rate of PDOC is assumed to be only 1/6 (K, Table 1) of the normal decomposition rate. Soil temperature used in the DOC production and mineralization is acquired by solving the soil heat transport equation (Sect. 2.2.2). These DOC processes are illustrated in Fig. 2.

2.3.2 DOC vertical movement

The vertical transport of DOC is modeled with the one-dimensional convection-dispersion equation:

$$\frac{\partial\left(\theta_{\mathrm{I}}C_{\mathrm{I}}''' + \theta_{\mathrm{L}}C'''\right)}{\partial t} = -\frac{\partial\left(qC'''\right)}{\partial z} + \frac{\partial\left(\theta_{\mathrm{L}}D\frac{\partial C'''}{\partial z}\right)}{\partial z} + P' + M' + S' + R' \quad (15a)$$

$$D = D_{\mathrm{dif}} + \lambda' \cdot \left|\frac{q}{\theta}\right| \quad (15b)$$

Where θ_{I} and θ_{L} are ice and liquid water content, respectively. t is the time (h), z is the soil depth (cm), C''' is the DOC concentration ($g\,mL^{-1}$), q is the vertical water flux density ($cm\,h^{-1}$), and D is the dispersion coefficient ($cm^2\,h^{-1}$). C_{I}''' is the DOC "concentration" in ice ($g\,mL^{-1}$). D_{dif} and λ' are the molecular diffusion coefficient ($cm^2\,h^{-1}$) and dispersivity (cm), respectively (Table 1). P', M' and S' describe DOC production, mineralization and sorption/desorption ($g\,cm^{-3}\,h^{-1}$) (Sect. 2.3.1 and Supplement D). R' is the DOC transfer rate from soil surface to overland flow (Sect. 2.4.3). By comparing Eq. (15) with Eq. (12), one may notice that we have assumed only DOC ($\theta_{\mathrm{L}}C'''$) can move in soil and PDOC ($\rho_{\mathrm{b}}S$) is attached on soil. In order to solve Eq. (15), it is necessary to know θ_{I}, θ_{L} and q which are obtained from solutions to the soil thermal and the Richards equations (Sect. 2.2). The boundary conditions for Eq. (15) are the specified fluxes, which are equal to the water flux times the DOC concentrations. Since DOC vertical movement normally occurs with spring floods when convective flow dominates infiltration, the overland DOC concentration can be used as the DOC concentration at

the upper boundary; DOC concentration at bottom is set as that of the bottom node. When freezing occurs, no mineralization, sorption, desorption, and transport of DOC were assumed until ice melts. More detailed steps are given in the Supplement D.

2.4 Flow routing and DOC transport

Overland flow can occur when the water depth on the ground surface exceeds the depression storage (Julien et al., 1995). In this study, overland flow is estimated in two dimensions using the continuity equation and the momentum equation with the diffusive wave approximation method. Channel flow is simulated in one dimension using the diffusive wave approximation method. The floodplain connection between overland cells and channels is also implemented. Water can move from the overland plane to the channel or vice versa according to the channel bank height and water surface elevation (Julien et al., 1995). Subsurface flow driven by the hydraulic gradient will enter the river when the water table is higher than water surface in channels.

2.4.1 Overland and channel flow

The governing equations for overland flow routing are based on the Saint–Venant equations of continuity and momentum. The full Saint–Venant equations can be simplified by using the diffusive wave approximation (Singh, 1996) which assumes that the net forces acting along the given axis of interest are zero with the continuity equation:

$$\frac{\partial h}{\partial t} + \frac{\partial q_x}{\partial x} + \frac{\partial q_y}{\partial y} = 0 \quad (16)$$

and the momentum equation:

$$S_{\mathrm{f}x} = S_{ox} - \frac{\partial h'}{\partial x} \quad (17a)$$

$$S_{\mathrm{f}y} = S_{oy} - \frac{\partial h'}{\partial y} \quad (17b)$$

Where h' is the surface flow depth (L), t is time, q_x and q_y are the unit flow rate in the x direction and y direction (L^2T^{-1}), respectively. e is the total throughfall and snow melt rate (LT^{-1}), and $S_{fx,y}S_{ox,y}$ are friction and bed slopes (unitless) in the x and y direction, respectively. h' is calculated in the infiltration module (Sect. 2.2.1). The flow resistance must be determined by solving overland flow equations. Assuming that flow is turbulent and the Manning formulation (in S.I. units) can describe the resistance:

$$q_{x,y} = a_{x,y} h'^{\beta} \tag{18a}$$

The Manning approximations for a_{xy} and β are:

$$a_{x,y} = \frac{S_{fx,y}^{1/2}}{n} \tag{18b}$$

$$\beta = \frac{5}{3} \tag{18c}$$

Where n is the Manning's overland roughness coefficient, which can by estimated from the land-use map (Woolhiser, 1975).

The channel flow routing process is modeled with one-dimensional diffusive channel flow equation (Julien and Saghafian, 1991), which is derived in a similar manner to its two-dimensional overland counterpart with the exception that channel flow routing only happens in a finite space established for a given channel section. The one-dimensional continuity relationship can be expressed with the following equation:

$$\frac{\partial A}{\partial t} + \frac{\partial Q}{\partial X} = q_{in} - q_{out} \tag{19}$$

Where A is the channel flow cross-section area (L^2); Q is channel discharge (L^3T^{-1}); q_{in} and q_{out} are lateral inflow and outflow per unit length (L^2T^{-1}), respectively. Furthermore, the flow within the channel is also assumed completely turbulent, and the

Manning's equation is used to estimate the channel discharge at a given time step:

$$Q = \frac{1}{n} A R^{\frac{2}{3}} s_f^{\frac{1}{2}} \tag{20}$$

Where R is the hydraulic radius (L); s_f is the friction slope (unitless) and n is the Manning roughness coefficient, respectively. Supplement E details the channel network building.

2.4.2 Saturated subsurface flow

The quasi- three-dimensional saturated subsurface flow model was used in this study. Each simulation cell can exchange water with its four adjacent neighbors. Local hydraulic gradients are approximated by local surface slopes. Therefore, a given grid will receive water from its upslope neighbors and discharge to its downslope neighbors. The subsurface routing method was not used for cells that contain perched water tables.

Under non-isothermal conditions, the effect of the ice layer on the subsurface flow should be considered. We used the soil profile of the two neighboring cells in order to illustrate our method (Fig. 3). The left column has one saturated zone whose thickness is H1, and its adjacent pixels shown in the right column may have four possible zones within the location of H1: top unsaturated layer (Z1), frozen saturated layer (Z2), liquid saturated layer (Z3) and bottom ice layer (Z4). One can deduce some relationships: $0 \le Z1 < H1$, $0 \le Z2 < H1$, $0 \le Z3 < H1$, $0 \le Z4 < H1$, $Z1 + Z2 + Z3 + Z4 = H1$.

The rate (L^3T^{-1}) of saturated subsurface flow from a specific cell to its down-gradient neighbors is modeled as:

$$Q_{i,j,d} = K_{i,j} \cdot D \cdot W' \cdot s \tag{21}$$

Where i, j are cell location indexes; d numbered from 0 to 7 represents directions between a cell and its eight adjacent eight neighbors; $Q_{i,j,d}$ is the flow rate (L^3/T) from

cell i, j in the d direction and W' is the width of flow in the d direction (L); $K_{i,j}$ (LT^{-1}) is the transmissivity at cell i, j; s is the slope gradient in the d direction and D is the acquifer thickness (L). D is estimated according to the location of the unsaturated zones in the neighbor cells, as well as the phase of the saturated layer under the unsaturated zone. Specifically, for the left soil column in scenario A in Fig. 3, its negihour cell has one ice layer (Z2) under the unsaturated zone (Z1). In this case, the acquifer (D) has its lower boundary at the top of Z2. In the scenario B, there is no Z2 layer. Thus, the lower boundary of the acquifer (D) is located at the top of the bottom ice layer (Z4). If there is no Z3 layer, the situation is similar to scenairo A. Finally, the acquifer thickness is the same as H1 if there is no Z2, Z3, Z4 at all.

2.4.3 Two-dimensional DOC transport

In the overland transport, DOC might be transported with the flow to a certain distance from its production sites but then re-accumulate at this new point if overland flow is not persistent enough for the DOC to reach a river channel. In surface overland DOC transport, we only consider the advection process. For two-dimensional flow in the overland plane, a continuity (conservation of mass) equation can be written as:

$$\frac{\partial(\rho_b S + \theta_L C'''_{ov})}{\partial t} = \frac{\partial(\boldsymbol{q}'_x \cdot C'''_{TOV})}{\partial x} + \frac{\partial(\boldsymbol{q}'_y \cdot C'''_{TOV})}{\partial y} + P' - M' + R' \tag{22}$$

Where C'''_{TOV} is the total DOC (DOC and PDOC) concentration in overland flow ($\mathrm{g\,mL^{-1}}$), C'''_{ov} is the DOC concentration in overland flow ($\mathrm{g\,mL^{-1}}$), t is the time, vector $\boldsymbol{q}$ $\{\boldsymbol{q}_x, \boldsymbol{q}_y\}$ is composed of overland flow flux density in the x and y direction ($\mathrm{cm\,s^{-1}}$), P' and M' are the microbial DOC production and mineralization rates ($\mathrm{g\,mL^{-1}\,s^{-1}}$), respectively (Sect. 2.3.1). Similarly, Eq. (22) is still applicable for DOC transport in channels except that its one-dimensional version is used. In overland DOC transport, we assumed both DOC (θC) and PDOC ($\rho_b S$) are carried with water. For overland water, the soil bulk density (ρ_b) is determined by the sediment concentration. In this study, we use

sediment concentration measured at the USGS gage station (USGS 15476000) to estimate the soil bulk density in overland flows (Supplement E). The DOC in soils may be transferred to surface runoff water (R'), especially during periods of heavy rainfall or snowmelt. The mass coefficient is related to a variety of hydrological factors including rain intensity and duration, slope and soils:

$$R' = k' \left[c'''(0) - C'''_{ov}\right] / \Delta z \tag{23}$$

Where k' is the transfer coefficient ($\mathrm{cm\,s^{-1}}$) and $c'''(0)$ is the DOC concentration at the soil surface. Equation (23) describes the rate-limited DOC transfer from the soil solution to the overland flow which is driven by the concentration gradient across the film layer that separates the stagnant soil solution and the moving overland flow (Wallach et al., 1988, 1989). The depth of the mixing zone (Δz) is normally very small (Zhang et al., 1997) and it is assumed to be 2 cm in this study. By assuming that overland flow is turbulent, we follow the method proposed by Wallach et al. (1989) to estimate k':

$$k' = \frac{D' \cdot n \cdot h'^{\frac{1}{3}} \cdot J^{\frac{1}{2}} \cdot \rho_L \cdot g}{\mu} \tag{24}$$

Where D' is the liquid diffusivity for DOC, n is the Manning roughness coefficient, h' is the overland water depth, J is the slope (fraction), ρ_L is the water density, g is the gravitational acceleration and μ is the viscosity coefficient.

The DOC transport in the subsurface system is assumed to only occur with ground water movement, and the dispersion effect, explained below, is not considered:

$$\frac{\partial\left(\theta_L C'''\right)}{\partial t} = \left(-Q_{sx} \cdot C''' - Q_{sy} \cdot C'''\right) / V \tag{25}$$

Where Q_{sx}, Q_{sy} are the saturated subsurface flow in the x and y directions ($\mathrm{L^3\,T^{-1}}$), respectively, estimated using the Darcy's law. V is the volume of one single simulation grid ($\mathrm{L^3}$). The subsurface DOC production, mineralization and sorption/desorption

processes are described in Sect. 2.3.2. We only considered the advection effect due to subsurface flows in DOC subsurface 2-dimensional horizontal transport. The DOC carried by subsurface flow will eventually reach a channel system when the water table is higher than the water surface of the channels. The q_x, q_y, q_{sx} and q_{sy} terms in Eqs. (22) and (25) are estimated by solving Eqs. (18) and (21).

2.5 Validation

Soil parameters (Ds, Ws, b_infilt) controlling runoff, infiltration and baseflow were adjusted to make the simulated hydrography match the observation at the outlet of our test watershed (see the Sect. 2.6). The comparison was documented in Supplement F. Because DOC concentrations are often measured for large river basins, it is difficult to parameterize the model for specific ecosystem types based on those measurements. Thus, we use the remotely-sensed DOC concentration data to parameterize the DOCDM 1.0. First, following the empirically-based algorithms in Griffin et al. (2011), the river DOC concentrations are estimated by using Landsat5 Thematic Mapper data on 18 July 2003 and 8 May 2004, respectively. Second, we compare our modeled DOC with the satellite-based estimates. Since the DOCDM 1.0 provides DOC channel concentrations on each hour, the model outputs that are closest to the satellite passing time are used for comparison. To spatially compare DOC concentrations from Landsat with the model results, remotely-sensed DOC concentrations are averaged into a 4 km resolution from the original 30 m (Supplement F).

Although the remotely-sensed DOC concentrations are overall higher than those from the simulation, the two datasets have a good relationship (Fig. 4; Supplement F), suggesting that the DOCDM 1.0 can capture the general trend of the watershed-level DOC yield. We are aware of that many parameters in the DOCDM 1.0 may introduce uncertainties and remotely-sensed results are also suffered from cloud contamination, observing angel, and the parameters in their retrieve method. For example, the overestimates in streamflow may be one of the reasons that result in low DOC concentrations in our simulations.

2.6 Case study region

To test the DOCDM 1.0, we choose a watershed in the Yukon River Basin as a case study (Fig. 5), The watershed is 6043 km^2 in size and its hydrological unit code (HUC) is 19040505. It is not significantly affected by the exterior stream sources and dominated by boreal forest and shrubland. The rectangle with dark outline in Fig. 5 is the channel network built from the elevation data. Each pixel on the channel has its own depth and width (not shown here). The land cover map is obtained from the University of Maryland's (UMD) 1 km Global Land Cover product (Hansen et al., 2000). Soil parameters (Nijssen et al., 2001a, b) and vegetation parameters including minimum stomatal resistance, albedo, and rooting depth are obtained from the VIC model website (http://www.hydro.washington.edu/Lettenmaier/Models/VIC/). The atmosphere forcing data, including precipitation, wind speed, maximum and minimum air temperature, used in the DOCDM 1.0 are acquired from NCEP reanalysis daily data (http://www.esrl.noaa.gov/psd/data/gridded/data.ncep.reanalysis.surfaceflux.html). All the input climate data originally have a daily time step and downscaled to an hourly time step using the MT-CLIM model (Kimball et al., 1997; Thornton et al., 1999) for the inputs to our land surface process module that operates on a 1 h time step. We run the DOCDM 1.0 for 1976 and 2004, which are the coldest and warmest years respectively since 1948.

3 Results and discussion

3.1 Point-level results

The location of our study pixel is denoted as the yellow point in Fig. 5. Its annual average air temperature for 2004 is −4.1 °C, compared to −5.3 °C in 1976. Its average summer (June–August) air temperature is 13.2 and 9.7 °C, respectively (Fig. 6). Its precipitation also shows an upward trend from 499.6 to 775.3 mm yr^{-1} during the

same period. The warmer and wetter condition led to thicker snow depth, earlier and more snow melting and thus deeper overland flow depth. Infiltration started immediately following the onset of snow melting. The relatively low infiltration rate in June and July was due to higher soil moisture and more incoming precipitation directly joined overland flow.

Soil temperature has increased (Fig. 7a) and active layer depth (ALD), the front of no-ice zone in Fig. 7b, became deeper, from 150 to 200 cm. Ice content will reach a peak at the beginning of snow melting when infiltration water refreezes at deeper soil layers (Fig. 7b). Infiltration also increases (Fig. 6e), possibly due to increasing water conductivity and deepening ALD. The DOC concentrations in liquid water (Fig. 7c) were accumulated around rooting zones in winter. Due to a deep snowpack, minimum vertical infiltration made DOC concentrations increase at a low rate. The relatively high surface (0–10 cm) soil temperature (−7.47 °C in 2004 vs. −8.94 °C in 1976) resulted in high DOC production in 2004. The DOC distribution in soils generally follows the rooting depth with low concentrations at mineral soil layers due to a limited amount of organic matter to support DOC production. When snow melts, DOC-enriched interstitial water in soils would be dramatically flushed out due to large vertical infiltration flow. Although warmer soils in summer may foster more DOC, the transfer into overland flow and also infiltration events largely kept DOC at a low level in soil profile. Since liquid water content is very low in winter, thus high DOC concentrations do not necessarily mean large DOC production (Fig. 7c). In contrast, there are three characteristics for DOC dynamics in summer: (1) high DOC production, (2) high DOC transport, and (3) low DOC concentrations in soils.

3.2 Watershed level results

The initial overland flow occurred on 8 June and 26 May in 1976 and 2004, respectively. The overland flow depths in three days after the initial overland events are shown (Fig. 8a and b). Overland flow depth was larger in 2004 than that in 1976. Also note that overland flow had a very shallow depth at nodes that contain slopes and channels.

It suggests that temperature, precipitation and catchment topography are the main factors controlling temporal and spatial trend of overland flow. The warming trend makes snow melting earlier. Deeper snowpack due to more precipitation results in higher overland flow. Pixels have channels or steep slopes have higher routing capacity and thus lower overland flow depth.

The DOC concentrations in overland flow on those two days were presented in Fig. 8c and d. Although more DOC stored during the winter of 2004 (Fig. 7c), more overland flow in 2004 diluted its DOC concentrations. Analysis for DOC concentrations in overland flow, land cover, and DEM (Fig. 5) shows that the different land cover types contributed differently to DOC concentrations. Specifically, the higher concentrations in downstream forests area suggested that forestland might have released more DOC into overland flow. On the other hand, shrubs disturbed at the upstream part of the watershed yielded less DOC. Many lines of evidence show that the rate of DOC production correlates well with the organic matter content in soils (Michalzik et al., 1999; Neff and Asner, 2001; Yurova et al., 2008). In the DOCDM 1.0, rooting depth is used to determine the amount of soil organic matter. Therefore, woody vegetation with deeper root has more DOC production than those with shallow root, such as shrubs and grass. The spatial pattern of overland DOC also indicated that topography is another important factor to consider. Pixels with larger compound topographic index (not shown), which is used to quantify the water convergence, tend to have higher DOC concentrations in the overland flow. The steep slopes make short ponding time, implying short contact time with organic-rich surface soil horizon, thus less soil DOC is transferred to overland flow. Meanwhile, flat areas will result in water-logged, thus anaerobic conditions that slow mineralization process, resulting in more DOC to be extracted from soils. No flush events before snow melt make a slow DOC accumulation in soils during winter. The maximum DOC concentration usually occures at the very beginning of the spring flood (See Fig. 8e and f) when long-term stored DOC is initially flushed. Since DOC is mainly distributed in surface soils and snow melting dominates overland water flow, more than half of annual DOC export is delievered during a brief snowmelt period

(around 4–7 weeks). After snow melting, rainfall barely resulted in overland events and its DOC concentration is low for the study region.

3.3 DOC trend and its environment factors

In the DOCDM 1.0, DOC can leave the watershed from three sources: overland (O), subsurface (S) and soil bottom (B). Water can be further removed by evapotranspiration (ET) in addition to the above three pathways. Water and DOC in overland and subsurface flow first route to channel and then to the river outlet eventually. Water and solute leak from soil bottom will enter the deeper ground layer and may reroute into channel system later. The groundwater in this study refers to both subsurface flow and bottom flow. Here we analyze how water and DOC distribute via those three pathways under changing environment conditions.

We define the annual infiltration ratio as the infiltration to precipitation in a given year. The higher infiltration ratio suggests the more dominant role of the groundwater system. Our simulations showed that the ratio increased from 0.27 to 0.42 during the study period (Fig. 9a). In other words, rainfall and snowmelt water have a larger tendency to join the subsurface, mainly due to increasing air temperature and deepening active layer (Fig. 7). Degrading permafrost increases hydrologic conductivity in soils, facilitating water infiltration.

Despite the increased groundwater, the ratio of overland DOC yield, defined as $DOC_O/(DOC_O + DOC_S + DOC_B)$, yet increased from 0.33 to 0.37 (Fig. 9b). The trend is out of expectation considering the decreasing role of surface transport (Fig. 9a). We believe that increasing soil temperature has two opposite effects on DOC yield. On the one hand, thawing soil makes less surface flow as shown above; on the other hand, increasing DOC production associated with higher soil temperature maintains overland flow as an important component in DOC transport. Although more water leaves the watershed from subsurface flow and bottom flow, relatively low soil temperature and poor organic matter content in deeper soil layers did not result in high DOC production. Therefore, DOC does not follow the recent warming trend. It is necessary to point out

that the above analysis depends on land cover types: DOC export through overland may have the similar decreasing trend on land covers with low organic matter content, such as tundra and bare land, since they do not have enough substrate to support DOC production even under warming conditions. These land covers unlikely have high DOC production and the DOC export via different pathways would primarily follow the pattern of hydrological regime.

The percentages of water flow via overland flow, subsurface flow, bottom flow and ET are shown in Fig. 9a. Decreasing ice due to warming led to increasing soil hydraulic conductivity and increased water leak from soil bottom. The large leak subsequently limited water supply to overland and subsurface flows. There was 43 % of water left the study region via belowground pathways in 2004, while the counterpart in 1976 was only 30 %. Thawing fosters soil moisture, but deeper active layer depth and larger infiltration make more water storage in the depth below the rooting system. Thus, ET is limited by moisture supply in shallow layers and low overland flow. As a result of these water flows, the DOC delivered through subsurface and bottom flow decreased from 68 to 61 %. The subsurface flow only took 1–2 % of the total water flux, but carried 30–50 % of DOC away. These dynamics are determined with two processes: (1) our horizontal subsurface flow takes place in active layer in which roots are distributed and have high DOC production. Therefore, subsurface flow usually has high DOC concentrations; and (2) the mixing zone in our model is set as 2 cm, which means overland flow can only extract DOC up to 2 cm depth in soils, thus the DOC in overland flow is low. The deeper mixing zone may provide higher fraction in overland DOC transport. From above analysis, flow volume is not the only factor to determine DOC yield; the physical and biological condition along flowpath is also essential to be considered. More water supplies to soil bottom will not conclusively indicate more DOC transport through groundwater movement.

We also listed the ratios of DOC sorption, mineralization and yield to DOC production for 1976 and 2004 in Table 2. The DOC yield here refers to the amount of DOC leaving the study watershed via both channel flow and bottom flow. Note that the DOC miner-

alization here includes the decomposition of both DOC and absorbed DOC. The fact that the absorbed DOC pool has ten times storage of the annual DOC production, suggesting it is necessary to take the sorption and desorption into account. The increasing soil moisture (liquid water) in the thawing months (May–September, not shown here) from 1976 to 2004 reduced DOC production, while the ratio of DOC mineralization to its production changed from 2.32 to 1.64, suggesting that the warming stimulated DOC production in soils. Meanwhile, the ratio of DOC yield to its production also showed a decreasing trend. The thawing soil and the associated hydrological alteration actually slowed down the DOC transport, resulting in more DOC accumulated in soils.

4 Conclusions

A catchment-scale DOC model is developed and applied for a watershed in Alaska. DOC flux and concentrations are found to be closely coupled with hydrological dynamics. We find that: (1) the snowmelt period (May–June) dominates the catchment's DOC export, (2) the permafrost thawing and enhancement in groundwater circulation contribute to river discharge in arctic and subarctic basins, (3) permafrost-driven changes in subsurface flow paths and water fluxes influence the flux of DOC from terrestrial to aquatic ecosystems; and (4) Increasing DOC production and more percolation water are two counterbalanced mechanisms in affecting DOC fluxes and concentrations under warming conditions. These dynamics might vary in different watersheds.

There are several limitations in this study. First, the initial condition of the model can induce uncertainty, especially when the simulation period is long. There is no available data as model initial conditions for large temporal scale simulations. Instead, in this study, we first run the VIC model for 10 years to generate an initial state for the DOCDM 1.0. This provides initial conditions for soil moisture and temperature. However, this may not be good way to get initial states for chemical-related variables. For instance, DOC, PDOC1 and PDOC2 are assumed to be zero at the beginning of the simulation. Second, as we have mentioned early, the lower boundary condition for the

water movement equation can significantly affect the hydrological dynamics, in turn, solute simulations. However, a trustable lower boundary condition requires extensive data for various variables. Third, parameters related to DOC production, mineralization, sorption and desorption are uncertain, and might have contributed to simulation uncertainty also. To improve parameterization, verify, and apply the model to the northern high latitudes in quantifying DOC dynamics, more data of DOC and its auxiliary physical, chemical and biological factors for various watersheds will be needed.

5 The hardware and software requirements and limitations

DOCDM 1.0 is written in C++ language and can be run in both Microsoft Windows and Linux environments. There is no special requirement for hardware and software to run DOCDM 1.0. All the input data can be readily acquired from internet. The main shortcoming for DOCDM 1.0 is that it is only suitable for relatively small watersheds. Because the lateral water transport is considered in DOCDM 1.0, memory should be allocated to all grid cells at the beginning of simulation, which limits the size of study watershed. In addition, since any given simulation grid cell requires the lateral flow from its neighbor cells, parallel computing is not easily to be implemented.

Code availability

The code is available under request for academic and non-commercial use. The code is also archived in our lab website (http://www.eaps.purdue.edu/ebdl/).

The Supplement related to this article is available online at doi:10.5194/gmdd-8-10411-2015-supplement.

Acknowledgements. This research is supported with projects funded to Q. Zhuang by NSF (DEB-0919331), the NSF Carbon and Water in the Earth Program (NSF-0630319), the NASA Land Use and Land Cover Change program (NASA-NNX09AI26G), Department of Energy (DE-FG02-08ER64599), the NSF Division of Information & Intelligent Systems (NSF-1028291), and DOE/Lawrence Berkeley National Laboratory IMPACTS Program. This research was also in part supported by the Director, Office of Science, Office of Biological and Environmental Research of the US Department of Energy under contract no. DE-AC02-05CH11231 as part of their Earth System Modeling Program.

References

Ågren, A., Haei, M., Köhler, S. J., Bishop, K., and Laudon, H.: Regulation of stream water dissolved organic carbon (DOC) concentrations during snowmelt; the role of discharge, winter climate and memory effects, Biogeosciences, 7, 2901–2913, doi:10.5194/bg-7-2901-2010, 2010.

Anderson, E. A.: A Point Energy and Mass Balance Model of a Snow Cover, NOAA Technical Report, US Dept. of Commerce, National Oceanic and Atmospheric Administration, National Weather Service, Office of Hydrology, Silver Spring, MD, 1976.

Andreadis, K. M., Storck, P., and Lettenmaier, D. P.: Modeling snow accumulation and ablation processes in forested environments, Water. Resour. Res., 45, W05429, doi:10.1029/2008WR007042, 2009.

Baker, M., Valett, M., and Dahm, C.: Organic carbon supply and metabolism in a shallow groundwater ecosystem, Ecology, 81, 3133–3148, doi:10.2307/177406, 2000.

Bowling, L. C., Pomeroy, J. W., and Lettenmaier, D. P.: Parameterization of blowing-snow sublimation in a macroscale hydrology model, J. Hydrometeorol., 5, 745–762, doi:10.1175/1525-7541(2004)005<0745:POBSIA>2.0.CO;2, 2004.

Boyer, E. B., Hornberger, G. M., Bencala, K. E., and McKnight, D. M.: Overview of a simple model describing variation of dissolved organic carbon in an upland catchment, Ecol. Model., 86, 183–188, doi:10.1016/0304-3800(95)00049-6, 1996.

Boyer, E. B., Hornberger, G. M., Bencala, K. E., and McKnight, D. M.: Effects of asynchronous snowmelt on the flushing of dissolved organic carbon: a mixing model approach,

Hydrol. Process., 18, 3291–3308, doi:10.1002/1099-1085(20001230)14:18<3291::AID-HYP202>3.0.CO;2-2, 2000.

Celia, M. A., Bouloutas, E. T., and Zarba, R. L.: A general mass-conservative numerical solution for the unsaturated flow equation, Water. Resour. Res., 26, 1483–1496, doi:10.1029/WR026i007p01483, 1990.

Cherkauer, K. A. and Lettenmaier, D. P.: Hydrologic effects of frozen soils in the upper Mississippi River Basin, J. Geophys. Res., 104, 19599–19610, doi:10.1029/1999JD900337, 1999.

Cherkauer, K. A. and Lettenmaier, D. P.: Simulation of spatial variability in snow and frozen soil, J. Geophys. Res., 108, 8858, doi:10.1029/2003JD003575, 2003.

Cherkauer, K. A., Bowling, L. C., and Lettenmaier, D. P.: Variable infiltration capacity cold land process model updates, Global Planet. Change, 38, 151–159, doi:10.1016/S0921-8181(03)00025-0, 2003.

Dickinson, R. E., Henderson-Sellers, A., Kennedy, P. J., and Wilson, M. F.: Biosphere–Atmosphere Transfer Scheme (BATS) for the NCAR Community Climate Model, NCAR Tech. Note TN-275+STR, National Center For Atmospheric Research, Boulder, CO, 1986.

Dittmar, T. and Kattner, G.: The biogeochemistry of the river and shelf ecosystem of the Arctic Ocean: a review, Mar. Chem., 83, 103–120, doi:10.1016/S0304-4203(03)00105-1, 2003.

Dutta, K., Schuur, E. A. G., Neff, J. C., and Zimov, S. A.: Potential carbon release from permafrost soils of northeastern Siberia, Global Change. Biol., 12, 2336–2351, doi:10.1111/j.1365-2486.2006.01259.x, 2006.

Fan, Z., Neff, J. C., and Wickland, K. P.: Modeling the production, decomposition, and transport of dissolved organic carbon in Boreal soils, Soil Sci., 175, 223–232, doi:10.1097/SS.0b013e3181e0559a, 2010.

Flerchinger, G. N. and Saxton, K. E.: Simultaneous heat and water model of a freezing snow-residue-soil system, I. Theory and development, T. ASAE, 32, 565–571, doi:10.13031/2013.31040, 1989.

Freeman, C., Evans, C. D., Monteith, D. T., Reynolds, B., and Fenner, N.: Export of organic carbon from peat soils, Nature, 412, 785, doi:10.1038/35090628, 2001.

Futter, M. N., Butterfield, D., Cosby, B. J., Dillon, P. J., Wade, A. J., and Whitehead, P. G.: Modeling the mechanisms that control in-stream dissolved organic carbon dynamics in upland and forested catchments, Water. Resour. Res., 43, W02424, doi:10.1029/2006WR004960, 2007.

Gorham, E.: Northern peatlands: role in the carbon cycle and probable responses to climatic warming, Ecol. Econ., 1, 182–195, doi:10.2307/1941811, 1991.
Griffin, C. G., Frey. K. E., Rogan, J., and Holmes, R. M.: Spatial and interannual variability of dissolved organic matter in the Kolyma River, east Siberia, observed using satellite imagery, J. Geophys. Res., 116, G03018, doi:10.1029/2010JG001634, 2011.
Hansen, M. C., DeFries, R. S., Townshend, J. R. G., and Sohlberg, R.: Global land covers classification at 1 km resolution using a classification tree approach, Int. J. Remote. Sens., 21, 1331–1364, doi:10.1080/014311600210209, 2000.
Hansson, K., Šimůnek, J., Mizoguchi, M., and Lundin, L. C.: Water flow and heat transport in frozen soil: numerical solution and freeze/thaw applications, Vadose Zone J., 3, 693–704, doi:10.2113/3.2.693, 2004.
Hinzman, L. D., Bettez, N. D., Bolton, W. R., Chapin, F. S., Dyurgerov, M. B., Fastie, C. L., Griffith, B., Hollister, R. D., Hope, A., Huntington, H. P., Jensen, A. M., Jia, G. J., Jorgenson, T., Kane, D. L., Klein, D. R., Kofinas, G., Lynch, A. H., Lloyd, A. H., McGuire, A. D., Nelson, F. E., Oechel, W. C., Osterkamp, T. E., Racine, C. H., Romanovsky, V. E., Stone, R. S., Stow, D. A., Sturm, M., Tweedie, C. E., Vourlitis, G. L., Walker, M. D., Walker, D. A., Webber, P. J., Welker, J. M., Winker, K. S., and Yoshikawa, K.: Evidence and implications of recent climate change in northern Alaska and other arctic regions, Climatic Change, 72, 251–298, doi:10.1007/s10584-005-5352-2, 2005.
Holmes, R. M., McClell, J. W., Raymond, P. A., Frazer, B. B., Peterson, B. J., and Stieglitz, M.: Lability of DOC transported by Alaskan rivers to the arctic ocean, Geophy. Res. Lett., 35, L03402, doi:10.1029/2007GL032837, 2008.
Hornberger, G. M., Bencala, K. E., and McKnight, D. M.: Hydrological controls on the temporal variation of dissolved organic carbon in the Snake River near Montezuma, Colorado, Biogeochemistry, 25, 147–165, doi:10.1007/BF00024390, 1994.
Johansen, O.: Thermal Conductivity of Soils, PhD thesis, Institute for Kjoletechnik, Trondheim, Norway, 1975.
Julien, P. Y. and Saghafian, B.: CASC2D User's Manual – A Two Dimensional Watershed Rainfall-Runoff Model, Colorado State University, Fort Collins, Fort Collins, CO, 1991.
Julien, P. Y., Saghafian, B., and Ogden, F. L.: Raster-based hydrologic modeling of spatially-varied surface runoff, Water Resour. Bull., 31, 523–536, doi:10.1111/j.1752-1688.1995.tb04039.x, 1995.

Kalbitz, K., Schwesig, D., Retnemeyer, J., and Matzer, E.: Stabilization of the dissolved organic matter by sorption to the mineral soil, Soil Biol. Biochem., 37, 1319–1331, doi:10.1016/j.soilbio.2004.11.028, 2005.
Karlstrom, H.: Peat Characteristics: Based on Multivariate Data Analysis of Magnetic Resonance Spectroscopy Data, Umea Univ., Umea, Sweden, 1995.
Kimball, J. S., Running, S. W., and Nemani, R.: An improved method for estimating surface humidity from daily minimum temperature, Agr. Forest Meteorol., 85, 87–98, doi:10.1016/S0168-1923(96)02366-0, 1997.
Liang, X., Lettenmaier, D. P., Wood, E. F., and Burges, S. J.: A simple hydrologically based model of land-surface water and energy fluxes for general-circulation models, J. Geophys. Res., 99, 14415–14428, doi:10.1029/94JD00483, 1994.
Lobbes, J. M., Fitznar, H. P., and Kattner, G.: Biogeochemical characteristics of dissolved and particulate organic matter in Russian rivers entering the Arctic Ocean, Geochim. Cosmochim. Acta, 64, 2973–2983, doi:10.1016/S0016-7037(00)00409-9, 2000.
Lu, X. L. and Zhuang, Q.: Areal changes of land ecosystems in the Alaskan Yukon River Basin from 1984 to 2008, Environ. Res. Lett., 6, 034012, doi:10.1088/1748-9326/6/3/034012, 2011.
Lundin, L. C.: Hydraulic properties in an operational model of frozen soil, J. Hydrol., 118, 289–310, doi:10.1016/0022-1694(90)90264-X, 1990.
Mei, Y., Hornberger, G. M., Kaplan, L. A., Denis, N. J., and Aufdenkampe, A. K.: Estimation of dissolved organic carbon contribution from hillslope soils to a headwater stream, Water. Resour. Res., 48, W09514, doi:10.1029/2011WR010815, 2012.
Michalzik, B. and Matzner, E.: Dynamics of dissolved organic nitrogen and carbon in a Central European Norway spruce ecosystem, Eur. J. Soil Sci., 50, 579–590, doi:10.1046/j.1365-2389.1999.00267.x, 1999.
Michalzik, B., Tipping, E., Mulder, J., Gallardo, L. J. F, Matzner, E., Bryant, C. L., Clarke, N., Lofts, S., and Vicente Esteban, M. A.: Modeling the production and transport of dissolved organic carbon in forest soils, Biogeochemistry, 66, 241–264, doi:10.1023/B:BIOG.0000005329.68861.27, 2003.
Monteith, J. L. and Unsworth, M. H.: Principles of Environmental Physics, 2nd edn., Routledge, Chapman and Hall, New York, 1990.
Moore, P. D.: The future of cool temperate bogs, Environ. Conserv., 29, 3–20, doi:10.1017/S0376892902000024, 2002.

Moore, T. R., Roulet, N. T., and Waddington. J. M.: Uncertainties in predicting the effect of climatic change on the carbon cycling of Canadian peatlands, Climatic Change, 40, 229–245, doi:10.1023/A:1005408719297, 1998.

Morris, D. P. and Hargreaves, B. R.: The role of photochemical degradation of dissolved organic carbon in regulating the UV transparency of 3 lakes on the Pocono Plateau, Limnol. Oceanogr., 42, 239–249, 1997.

Neff, J. C. and Asner, G. P.: Dissolved organic carbon in terrestrial ecosystems: synthesis and a model, Ecosystems, 4, 29–48, doi:10.1007/s100210000058, 2001.

Nijssen, B., O'Donnell, G. M., Hamlet, A. F., and Lettenmaier, D. P.: Hydrologic sensitivity of global rivers to climate change, Climatic Change, 50, 143–175, doi:10.1023/A:1010616428763, 2001a.

Nijssen, B., O'Donnell, G. M., Lettenmaier, D. P., Lohmann, D., and Wood, E. F.: Predicting the discharge of global rivers, J. Climate, 14, 3307–3323, doi:10.1175/1520-0442(2001)014<3307:PTDOGR>2.0.CO;2, 2001b.

Patankar, S. V.: Numerical Heat Transfer and Fluid Flow, Computational Methods in Mechanics and Thermal Science Series, Hemisphere, New York, 1980.

Qualls, R. G. and Haines, B. L.: Geochemistry of dissolved organic nutrients in water percolating through a forest ecosystem, Soil Sci. Soc. Am. J., 55, 1112–1123, 1991.

Qualls, R. G. and Haines, B. L.: Biodegradability of dissolved organic matter in forest throughfall, soil solution, and stream water, Soil Sci. Soc. Am. J., 56, 578–586, 1992a.

Qualls, R. G. and Haines, B. L.: Measuring adsorption isotherms using continuous, unsaturated flow through intact soil cores, Soil Sci. Soc. Am. J., 56, 456–460, 1992b.

Raymond, P. A. and Bauer, J. E.: Bacterial consumption of DOC during transport through a temperate estuary, Aquat. Microb. Ecol., 22, 1–12, doi:10.3354/ame022001, 2000.

Raymond, P. A., McClelland, J. W., Holmes, R. M., Zhulidov, A. V., Mull, K., Peterson, B. J., Striegl, R. G., Aiken, G. R., and Gurtovaya, T. Y.: Flux and age of dissolved organic carbon exported to the Arctic Ocean: a carbon isotopic study of the five largest arctic rivers, Global Biogeochem. Cy., 21, GB4011, doi:10.1029/2007GB002934, 2007.

Reeve, A. S., Siegel, D. I., and Glaser, P. H.: Simulating vertical flow in large peatlands, J. Hydrol., 227, 207–217, doi:10.1016/S0022-1694(99)00183-3, 2001.

Richards, L. A.: Capillary conduction of liquids through porous mediums, Physics, 1, 318–333, 1931.

Serreze, M. C., Walsh, J. E., Chapin III, F. S., Osterkamp, T., Dyurgerov, M., Romanovsky, V., Oechel, W. C., Morison, J., Zhang, T., and Barry, R. G.: Observational evidence of recent change in the northern high-latitude environment, Climatic Change, 46, 159–207, doi:10.1023/A:1005504031923, 2000.

Singh, V. P.: Kinematic wave modeling in water resources: surface water hydrology, Wiley-Interscience, New York, 1996.

Storck, P., Lettenmaier, D. P., and Bolton, S. M.: Measurement of snow interception and canopy effects on snow accumulation and melt in a mountainous maritime climate, Oregon, United States, Water. Resour. Res., 38, 1223, doi:10.1029/2002WR001281, 2002.

Striegl, R. G., Aiken, G. R., Dornblaser, M. M., Raymond, P. A., and Wickland, K. P.: A decrease in discharge-normalized DOC export by the Yukon River during summer through autumn, Geophys. Res. Lett., 32, L21413, doi:10.1029/2005GL024413, 2005.

Tarboton, D. G., Chowdhury, T. G., and Jackson, T. H.: A spatially distributed energy balance snowmelt model, in: Biogeochemistry of Seasonally Snow Covered Catchments, edited by: Tonneson, K. A. et al., International Association of Hydrological Sciences, Boulder, CO, 141–155, 1995.

Thornton, P. E. and Running, S. W.: An improved algorithm for estimating incident daily solar radiation from measurements of temperature, humidity, and precipitation, Agr. Forest Meteorol., 93, 211–228, doi:10.1016/S0168-1923(98)00126-9, 1999.

Tranvik, L. J. and Jansson, M.: Terrestrial export of organic carbon, Nature, 415, 861–862, doi:10.1038/415861b, 2002.

Van Genuchten, M. T.: A closed-form equation for predicting the hydraulic conductivity of unsaturated soils, Soil Sci. Soc. Am. J., 44, 892–898, doi:10.2136/sssaj1980.03615995004400050002x, 1980.

van Genuchten, M. T. and Wagenet, R. J.: Two-site/two-region models for pesticide transport and degradation: theoretical development and analytical solutions, Soil Sci. Soc. Am. J., 53, 1303–1310, doi:10.2136/sssaj1989.03615995005300050001x, 1989.

Wallach, R., Jury, W. A., and Spencer, W. F.: Transfer of chemicals from soil solution to surface runoff: a diffusion-based soil model, Soil Sci. Soc. Am. J., 52, 612–618, doi:10.2136/sssaj1988.03615995005200030002x, 1988.

Wallach, R., Jury, W. A., and Spencer, W. F.: The concept of convective mass transfer for prediction of surface-runoff pollution by soil surface applied chemicals, T. ASAE, 32, 906–912, doi:10.13031/2013.31089, 1989.

Woolhiser, D. A.: Simulation of unsteady overland flow, in: Unsteady Flow in Open Channels, edited by: Mahmood, K. and Yevjevich, V., Fort Collins, Colorado, 485–508, 1975.
Xu, N. and Saiers, J. E.: Temperature and hydrologic controls on dissolved organic matter mobilization and transport within a forest topsoil, Environ. Sci. Technol., 44, 5423–5429, doi:10.1021/es1002296, 2010.
Yurova, A., Sirin, A., Buffam, I., Bishop, K., and Laudon, H.: Modeling the dissolved organic carbon output from a boreal mire using the convection-dispersion equation: importance of representing sorption, Water. Resour. Res., 44, W07411, doi:10.1029/2007WR006523, 2008.
Zhang, X. C., Norton, C. D., and Nearing, M. A.: Chemical transfer from soil solution to surface runoff, Water. Resour. Res., 33, 809–815, doi:10.1029/96WR03908, 1997.

Table 1. The parameters and constants used in models of DOC production, minearlization and sortpion and desortion.

Symbol	Value	Units	Description	Source
Q_{10}	1.7	–	The effect of temperature on DOC production and mineralization	Yurova et al. (2008)
P_{basal}	$0.4–2.4 \times 10^{-3}$	$mg\,g^{-1}\,h^{-1}$	Microbial DOC production at 20 °C	Yurova et al. (2008) and also see the Supplement C
M_{basal}	0.4×10^{-4}	h^{-1}	DOC mineralization rate at 20 °C	Yurova et al. (2008)
f	0.317	–	Fraction of exchange sites in equilibrium with the type 1 PDOC	Fan et al. (2010)
K_d	0.136	$mL\,g^{-1}$	The linear partition coefficient between the solid and aqueous phases	Fan et al. (2010)
a	0.274	h^{-1}	Maximum mass transfer coefficient	Fan et al. (2010)
K	1/6	fraction	The constant reducing the microbial mineralization rate when the soluble DOC is sorbed	Kalbitz et al. (2005)
K_{anp}	0.07	–	Ratio of anaerobic to aerobic DOC production	Yurova et al. (2008)
D_{dif}	4.3×10^{-2}	$cm^2\,h^{-1}$	Molecular diffusion coefficient	Karlstrom (1995)
λ'	10	cm	Dispersivity	Reeve et al. (2001)

Table 2. The ratios of DOC prodction to its sorption, mineralization and transport in 1976 and 2004.

Ratios	1976	2004
$\frac{DOC_{production}}{DOC_{sorption}}$	8.68 %	5.25 %
$\frac{DOC_{production}}{DOC_{mineralization}}$	42.92 %	60.95 %
$\frac{DOC_{production}}{DOC_{transport}}$	74.45 %	161.50 %

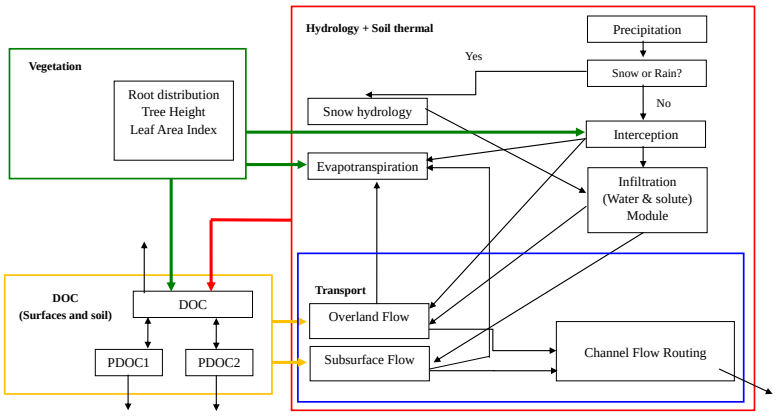

Figure 1. DOCDM 1.0 framework of hydrology, vegetation and DOC dynamics. See Supplement A for more details of description. The processes of DOC dynamics (yellow part) are further illustrated in Fig. 2.

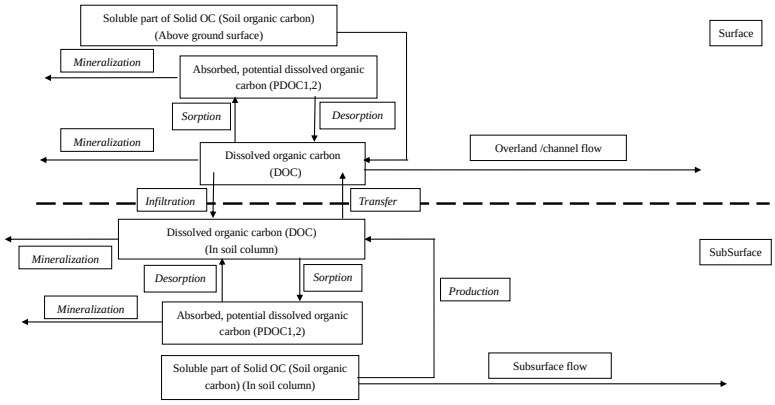

Figure 2. Schematic diagram of the pools of soluble organic matter (DOC and PDOC) and production, mineralization and adsorption and desorption processes (the yellow part in Fig. 1).

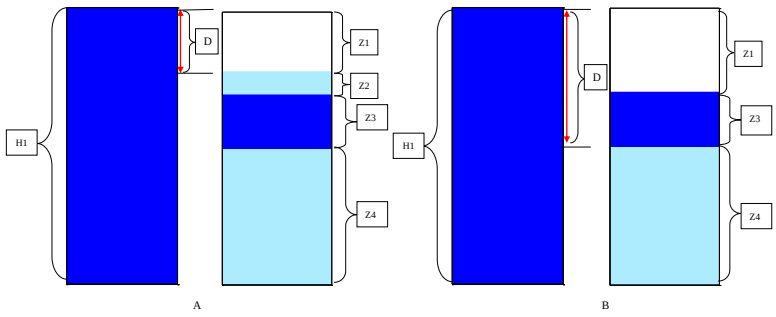

Figure 3. The two scenarios for the saturated subsurface flow between adjacent neighbors. Grey, blue and white represent ice, liquid saturated and unsaturated regions in soil column, respectively. H1: saturated layer in soil column. Z1: possible top unsaturated layer. Z2: possible ice layer. Z3: possible liquid saturated layer. Z4: possible bottom ice layer. *D*: effective acquifer thickness.

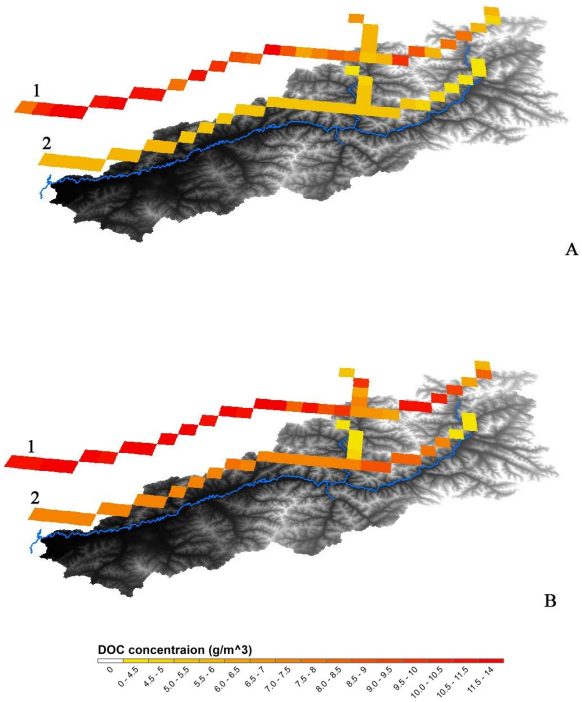

Figure 4. The DOC validation results for days of 18 July 2003 **(a)** and 5 August 2004 **(b)**. Numbers 1 and 2 stand for the satellite observation and simulations, respectively. The river network and elevation are also displayed as background.

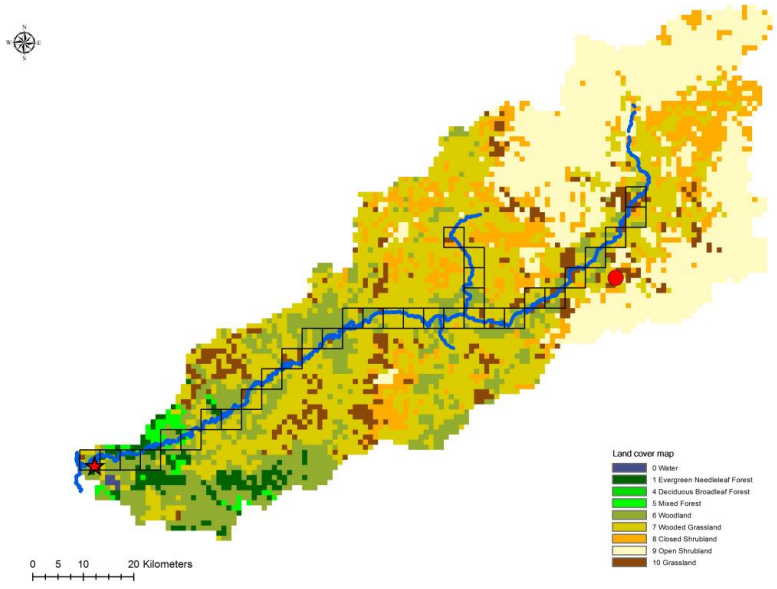

Figure 5. The land cover map for the test watershed (HUC 19040405). The red star stands for the river outlet and the red soild cicrle is the demonstration point. The resolution for this map is 1 km. The simulation grids (4 km in this study) with dark outline have the river channel in them.

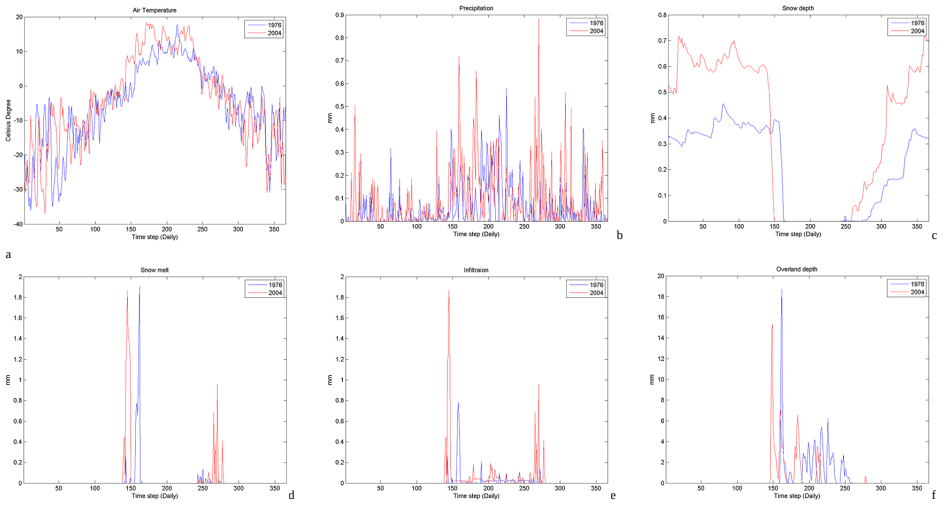

Figure 6. The model outputs on the demonstraion point in 1976 and 2004: **(a)** air temperaure **(b)** precipitatin **(c)** snow depth **(d)** snowmelt **(e)** infiltration and **(f)** overland depth.

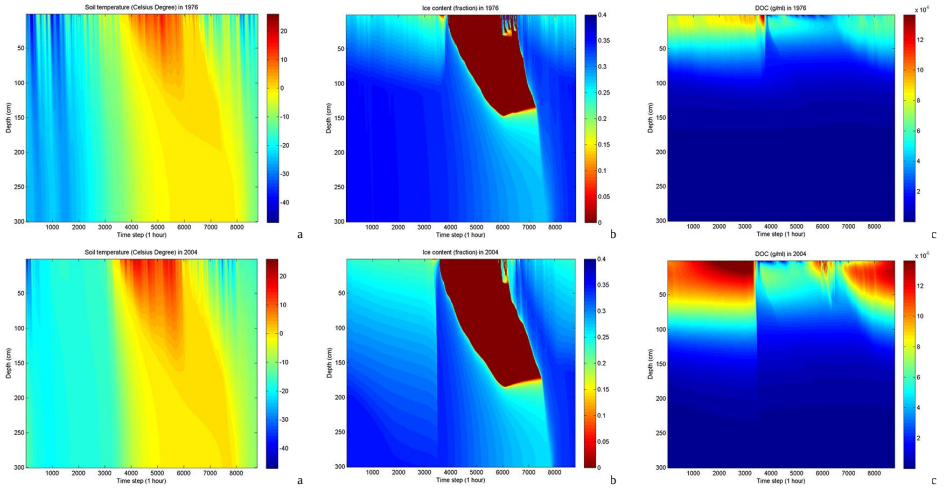

Figure 7. The model outputs in 1976 and 2004: **(a)** soil temperature **(b)** ice content and **(c)** DOC concentration profile. The time step is one hour.

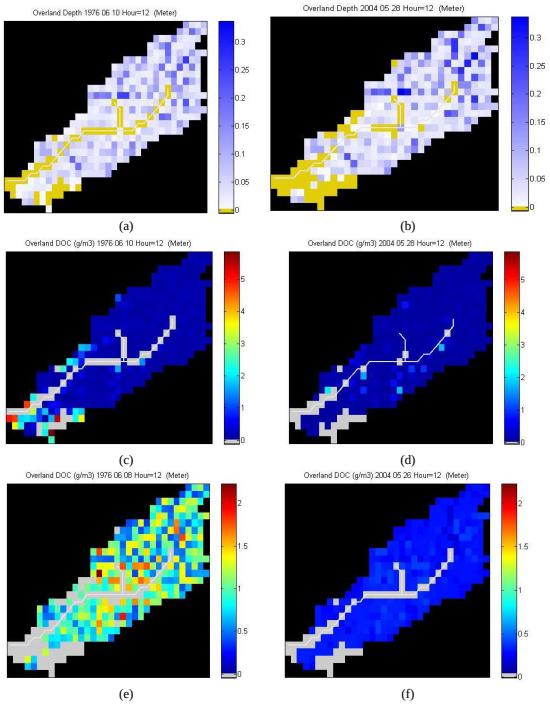

Figure 8. The overland flow depth on 10 June 1976 **(a)**, 27 May 2004 **(b)** and the DOC concentration in overland flow on the two days **(c, d)**; the time is 12.00 a.m.

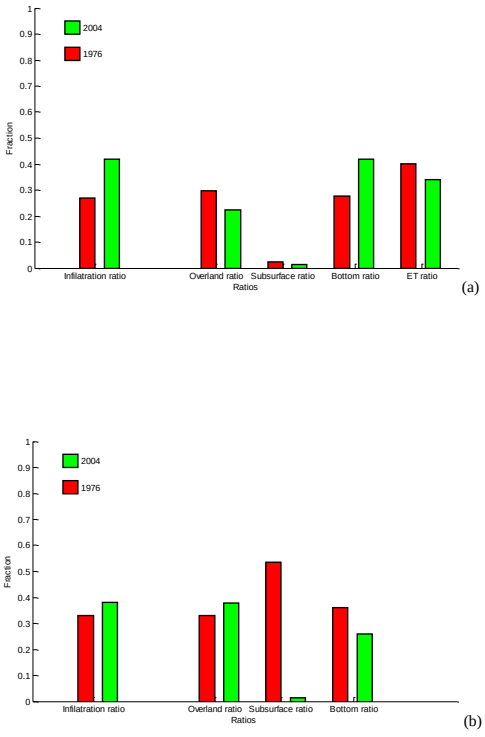

Figure 9. The change of water **(a)** and DOC **(b)** infilatrion ratio and their transport pathways in 1976 and 2004.